

Cis–Trans Isomerization in Crystalline $[(\eta^5\text{-C}_5\text{H}_5)\text{Fe}(\mu\text{-CO})(\text{CO})]_2$

Dario Braga,^{*,†} Michele R. Chierotti,[‡] Nadia Garino,[‡] Roberto Gobetto,^{*,‡}
Fabrizia Grepioni,[†] Marco Polito,[†] and Alessandra Viale[‡]

Dipartimento di Chimica G. Ciamician, Università di Bologna, Via F. Selmi 2, 40126 Bologna, Italy, and
Dipartimento di Chimica I.F.M., Università di Torino, Via P. Giuria 7, 10125 Torino, Italy

Received December 4, 2006

The *cis–trans* isomerization of $[(\eta^5\text{-C}_5\text{H}_5)\text{Fe}(\mu\text{-CO})(\text{CO})]_2$, well known in solution, has been studied also in the solid state. The solid-state process has been investigated on polycrystalline samples by ^{13}C CPMAS NMR spectroscopy and variable-temperature powder diffraction (VTXPD). It has been shown that an irreversible isomerization takes place at 80 °C. The reaction was also monitored by heating the sample at four different temperatures for periods of time and by determining the conversions by a ^{13}C CPMAS spectrum. The transformation has been shown to obey a first-order Avrami–Erofe'ev rate law typical of a nucleation and growth mechanism. By the Sharp–Hancock plot of the isotherms it has been demonstrated that the process is not isokinetic, and the Avrami exponentials indicate that it passes from a one- to a three-dimensional growth. An activation energy of 164 ± 7 kJ/mol for the isomerization process has been found.

Introduction

Intermolecular interactions play a central role in many chemical transformations.¹ It has been demonstrated, for example, that the effect of different solvents on the transition-state energy can heavily modify rates and reaction mechanisms.² Reactions that take place within a crystal,³ where solvent–molecule interactions are absent, represent a special case. Indeed the constrained environment of the crystal packing controls the reaction paths⁴ and limits the number of accessible transition-state structures, which are otherwise available in solution. Such selection often leads to the formation of products that differ from those obtained in solution, affording new synthetic opportunities.

Even though the topochemical principle has been met with some scepticism,⁵ the possibility of controlling solid-state reactions by controlling the crystal packing is one of the most fascinating fields of supramolecular chemistry.⁶

The understanding of a solid-state transformation requires also an appreciation of the kinetics of the reaction. However, a solid-state kinetic study is a challenging task because the loss of the 3-D order during reaction makes the appreciation of the reaction mechanism very difficult. There are examples⁷ of reactions that occur without loss of the 3-D order such as the single-crystal to single-crystal reactions. In these cases it is possible to obtain information on the structure of the transition state by means of techniques such as X-ray and neutron crystallography.⁸

Several other solid-state techniques can be of great help in the evaluation of the kinetics of transformations taking place in the solid state. Among them, high-resolution solid-state NMR (SS NMR) and powder diffraction techniques appear to be particularly well suited to investigate solid systems lacking extensive order or homogeneity for the breakdown of the original 3-D order.

A large number of studies dealing with kinetics of solid-state processes are available in the literature. These are mainly dedicated to the polymorphic transformations of crystalline solids, a central topic in the pharmaceutical industry.⁹ The problem is not simple at all if one considers that within the lattice molecules do not have an equal probability of undergoing a chemical reaction.^{10–14} Thus, the reaction may occur with different activation energies depending on the spatial location of reactants.

* To whom correspondence should be addressed. E-mail: roberto.gobetto@unito.it and dario.braga@unibo.it.

[†] Dipartimento di Chimica G. Ciamician, Università di Bologna.

[‡] Dipartimento di Chimica I.F.M. Università di Torino.

(1) (a) Lehn, J. M. *Angew. Chem., Int. Ed. Engl.* **1990**, *29*, 1304–1319. (b) Lehn, J. M. *Supramolecular Chemistry: Concepts and Perspectives*, VCH: Weinheim, 1995. (c) Steed, J. W.; Atwood, J. L. *Supramolecular Chemistry*; Wiley & Sons: New York, 2000.

(2) (a) Atwood, J. D. *Inorganic and Organometallic Reaction Mechanisms*; Brooks/Cole: Belmont, CA, 1985. (b) Carrion, M. C.; Guerrero, A.; Jalon, F. A.; Manzano, B. R.; De la Hoz, A.; Claramunt, R. M.; Milata, V.; Elguero, J. *Inorg. Chem.* **2003**, *42*, 885–895.

(3) (a) Braga, D.; Grepioni, F. *Angew. Chem., Int. Ed.* **2004**, *43*, 2–7. (b) Braga, D.; Grepioni, F. *Top. Curr. Chem.* **2005**, *254*, 71. (c) Trask, A. V.; Jones, W. *Top. Curr. Chem.* **2005**, *254*, 41. (d) Kaupp, G. *Top. Curr. Chem.* **2005**, *254*, 95.

(4) (a) Coville, N. J.; Cheng, L. *J. Organomet. Chem.* **1998**, *571*, 149–169. (b) Coville, N. J.; Levendis, D. C. *Eur. J. Inorg. Chem.* **2002**, *12*, 3067–3078. (c) Adeyemi, A. G.; Eke, U. B.; Cheng, L.; Cook, L. M.; Billing, D. G.; Mamba, B. B.; Levendis, D. C.; Coville, N. J. *J. Organomet. Chem.* **2004**, *689*, 2207–2215. (d) Horwood, O. P. M.; Billing, D. G.; Levendis, D. C.; Nareetsile, F. M.; Coville, N. J. *CrystEngComm* **2003**, *5*, 468–473.

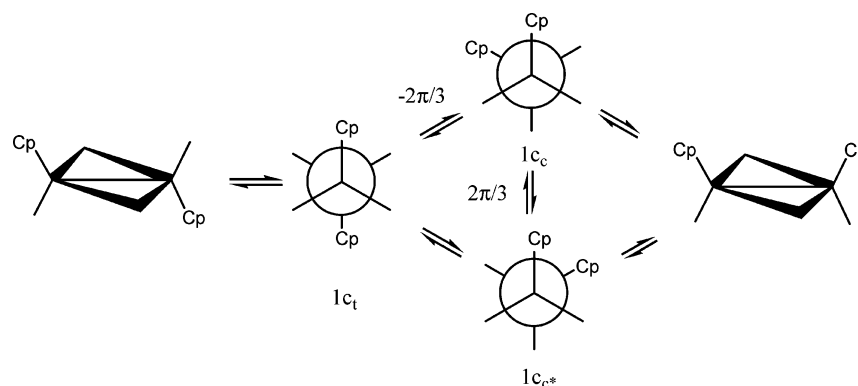
(5) (a) Cohen, M. D.; Schmidt, G. M. J. *J. Chem. Soc.* **1964**, 1996. (b) Cohen, M. D. *Angew. Chem., Int. Ed. Engl.* **1975**, *14*, 386–394. (c) Kaupp, G. In *Comprehensive Supramolecular Chemistry*; Davies, J. E. D., Ed.; Elsevier: Oxford, 1996; Vol. 8, p 381.

(6) (a) MacGillivray, L. R. *CrystEngComm* **2000**, *2*, 1, and references therein. (b) Papaefstathiou, G. S.; Kipp, A. J.; MacGillivray, L. R. *Chem. Commun.* **2001**, 2462–2463. (c) Papaefstathiou, G. S.; MacGillivray, L. R. *Angew. Chem., Int. Ed.* **2002**, *41*, 2070. (d) Frišćić, T.; MacGillivray, L. R. *Chem. Commun.* **2003**, 1306–1307. (e) Gao, X.; Frišćić, T.; MacGillivray, L. R. *Angew. Chem., Int. Ed.* **2004**, *43*, 232–236. (f) Cave, G. W. V.; Raston, C. L.; Scott, J. L. *Chem. Commun.* **2001**, 2159.

(7) (a) Ohhara, T.; Harada, J.; Ohashi, Y.; Tanaka, I.; Kumazawa, S.; Niimura, N. *Acta Crystallogr.* **2000**, *B56*, 245–253. (b) Ohashi, Y. *Acc. Chem. Res.* **1988**, *21*, 268–274. (c) Sekine, A.; Tatsuki, H.; Ohashi, Y. *J. Organomet. Chem.* **1997**, *389*, 536–537.

(8) Bogadi, R. S.; Levendis, D. C.; Coville, N. J. *J. Am. Chem. Soc.* **2002**, *124*, 1104–1110.

(9) (a) McCrone, W. C. *Polymorphism in Physics and Chemistry of the Organic Solid State*; Fox, D., Labes, M. M. A., Eds.; Weissenberg, Interscience: New York, 1965; Vol. II, p 726. (b) Bernstein, J. *Polymorphism in Molecular Crystals*; Oxford University Press: Oxford, 2002.

Scheme 1. *Cis-Trans* Isomerization of $[(\eta^5\text{-C}_5\text{H}_5)\text{Fe}(\mu\text{-CO})(\text{CO})_2]$ 

In this work we combine spectroscopic (SS NMR) and diffraction (variable-temperature XPD) experiments to investigate the solid-state isomerization process of *cis/trans*- $[(\eta^5\text{-C}_5\text{H}_5)\text{Fe}(\mu\text{-CO})(\text{CO})_2]$, a classical textbook case of structurally nonrigid organometallic complexes in solution.

$[(\eta^5\text{-C}_5\text{H}_5)\text{Fe}(\mu\text{-CO})(\text{CO})_2]$ is known to exist in two isomers: in the *cis* form the two cyclopentadienyl rings are on the same side of the plane defined by the iron atoms and the two bridging carbonyls, while in the *trans* one they are on opposite sides (Scheme 1).

In solution the interconversion between the two isomers is very fast and brings to an equilibrium mixture of the two species. Because bridging–terminal carbonyl exchange is rapid for the *trans* isomer at all accessible temperatures, at ambient temperature a single averaged carbonyl resonance is observed. The variable-temperature study of carbonyl fluxionality in $[(\eta^5\text{-C}_5\text{H}_5)\text{Fe}(\mu\text{-CO})(\text{CO})_2]$ is one of the best known examples of ligand exchange processes involving complexes containing metal–metal bonds in solution.^{15–18} Adams and Cotton proposed an interconversion mechanism involving an intermediate “all-terminal” species containing only terminal carbonyls: whether the *cis* or *trans* isomer is obtained depends upon the $\text{FeCp}(\text{CO})_2$ unit rotation around the Fe–Fe axis in this intermediate. The same type of rotation leads to a bridging–terminal carbonyl exchange. Farrugia and Mustoo¹⁹ observed that this exchange process is fast in the *trans* isomer (the kinetic constants of the exchange and isomerization processes are comparable), but not in the *cis* one.

Both *cis* and *trans* isomers of $[(\eta^5\text{-C}_5\text{H}_5)\text{Fe}(\mu\text{-CO})(\text{CO})_2]$ can be separately crystallized, and solid-state ¹³C NMR studies show

that the carbonyl ligands are not dynamic at any accessible temperature.²⁰ The single-crystal structures were determined by Bryan and Greene in 1970. The reader is referred to these seminal studies for the comparison of the single-crystal structures of the two compounds.²¹

The reorientational motion of the cyclopentadienyl ligands in the crystal structures of the two complexes has also been investigated by packing potential energy calculations.²² Recently, some of us reported an investigation of the dynamics of $[(\eta^5\text{-C}_5\text{H}_5)\text{Fe}(\mu\text{-CO})(\text{CO})_2]$ included in γ -cyclodextrin in the solid state.²³ The study showed that the microenvironment provided by the inclusion cavity allows much more extensive dynamic rearrangements of the guest molecules, in comparison to pure *cis*- or *trans*- $[(\eta^5\text{-C}_5\text{H}_5)\text{Fe}(\mu\text{-CO})(\text{CO})_2]$. Inside the cyclodextrin the *trans* isomer undergoes rapid bridge–terminal carbonyl exchange even at 100 K. The dynamics in the solid state inclusion environment shows modified rates of the exchange processes compared to those detected in solution. For example, the rate of bridge–terminal carbonyl exchange in the *cis* isomer is greater than the rate of *cis*–*trans* isomerization.

Now we are interested in investigating the kinetics of the *cis*–*trans* transformation in the solid state by the combined use of high-resolution ¹³C CPMAS NMR spectroscopy and X-ray powder diffraction (XRPD) techniques.

Our aim is to address the following questions:

What is the composition of the *cis*–*trans* mixture at the end of the transformation process?

What is the mechanism of the isomerization in the solid state?

What is the value of the activation energy of the *cis*–*trans* interconversion in the solid state?

Is the solid-state isomerization process different from that in solution?

Results and Discussion

We will first describe the results of the cross-polarization magic-angle spinning ¹³C CPMAS NMR experiments and then proceed with a description of the variable-temperature X-ray diffraction experiments.

(10) Young, D. A. *Decomposition of Solids*; Pergamon Press: Oxford, 1966.

(11) Garner, W. E. *Chemistry of the Solid State*; Butterworths: London, 1955.

(12) O'Brien, P. *Polyhedron* **1983**, *2*, 233.

(13) Ng, W. L. *Austr. J. Chem.* **1977**, *28*, 1169.

(14) Skrdla, P. J.; Robertson, R. T. *J. Phys. Chem. B* **2005**, *109*, 10611.

(15) (a) Bullitt, J. G.; Cotton, F. A.; Marks, T. J. *J. Am. Chem. Soc.* **1970**, *92*, 2155–2156. (b) Bullitt, J. G.; Cotton, F. A.; Marks, T. J. *Inorg. Chem.* **1972**, *11*, 671–676. (c) Adams, R. D.; Cotton, F. A. *J. Am. Chem. Soc.* **1973**, *95*, 6589–6594. (d) Cotton, F. A.; Hanson, B. E. In *Rearrangements in Ground and Excited States*; De Mayo, P., Ed.; Academic Press: New York, 1980; p 379.

(16) Gansow, A. G.; Burke, A. R.; Vernon, W. D. *J. Am. Chem. Soc.* **1976**, *94*, 2551–2552.

(17) Harris, D. C.; Rosenberg, E.; Roberts, J. D. *J. Chem. Soc., Dalton Trans.* **1974**, 2398.

(18) Gansow, A. G.; Burke, A. R.; Vernon, W. D. *J. Am. Chem. Soc.* **1976**, *98*, 5817–5826.

(19) (a) Farrugia, L. J.; Mustoo, L. *Organometallics* **1992**, *11*, 2941–2944. (b) Farrugia, L. J. *J. Chem. Soc., Dalton Trans.* **1997**, 1785. (c) Gansow, O. A.; Burke, A. R.; Vernon, W. D. *J. Am. Chem. Soc.* **1976**, *98*, 5817.

(20) (a) Aime, S.; Botta, M.; Gobetto, R.; Orlandi, A. *Magn. Reson. Chem.* **1990**, *28S*, 52–58. (b) Aime, S.; Dastrù, W.; Gobetto, R.; Hawkes, G. E. *Advanced Applications of NMR to Organometallic Chemistry*; John Wiley and Sons: New York, 1996.

(21) (a) Bryan, R. F.; Greene, P. T.; Newlands, M. J.; Field, D. J. *J. Chem. Soc. A* **1970**, 3068. (b) Bryan, R. F.; Greene, P. T. *J. Chem. Soc. A* **1970**, 3064.

(22) (a) Braga, D.; Gradella, C.; Grepioni, F. *J. Chem. Soc., Dalton Trans.* **1989**, 1721. (b) Braga, D. *Chem. Rev.* **1992**, *92*, 633.

(23) Canuto, H. C.; Masic, A.; Rees, N. H.; Heyes, S. J.; Gobetto, R.; Aime, S. *Organometallics* **2006**, *25*, 2248–2252.

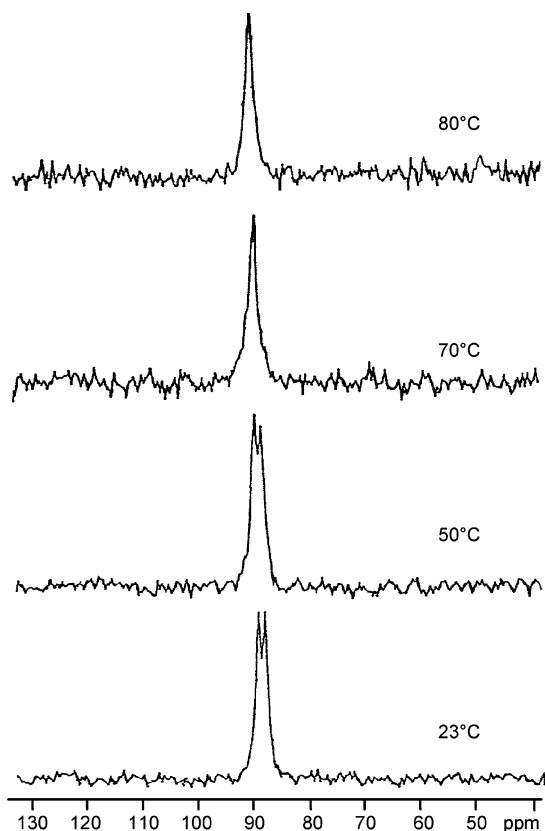


Figure 1. Cyclopentadienyl rings region of the ^{13}C CPMAS NMR spectra of $\text{cis}-[(\eta^5\text{-C}_5\text{H}_5)\text{Fe}(\mu\text{-CO})(\text{CO})]_2$ recorded at variable temperature.

In Figure 1 the variable-temperature ^{13}C CPMAS NMR spectra of $\text{cis}-[(\eta^5\text{-C}_5\text{H}_5)\text{Fe}(\mu\text{-CO})(\text{CO})]_2$, in the region of the cyclopentadienyl rings' chemical shifts, are reported. At 23 °C, as expected, the two rings in the *cis* isomer are not equivalent and give rise to two different peaks at 88.5 and 90.5 ppm. Indeed, it is known that they are crystallographically different,²¹ and moreover they have different activation energies (E_a) for the rotation.²² By raising the temperature to 80 °C, the progressive formation of the *trans* isomer, having the two rings symmetrically equivalent, is confirmed by the presence of a single resonance at 92.0 ppm.

It is interesting to observe that, unlike in the solution case, in the solid state the *cis*–*trans* conversion is complete and not reversible: the more stable *trans* isomer is the only species observed at the end of the process even after cooling the sample to 25 °C. As expected, no formation of the *cis* isomer can be detected by heating a sample of pure *trans* isomer to 80 °C. Then we must conclude that in the solid state the two isomers are separated by a larger free energy of formation than in solution, and this phenomenon must be associated with the presence of intermolecular forces in the crystalline environment that are able to stabilize the *trans* isomer. Likely the *cis* isomer is destabilized in the solid state for the higher dipole moment compared to the *trans* isomer.

The same process can be monitored by recording ^{13}C CPMAS spectra of the *cis* isomer heated for increasing times. The decrease of the *cis* isomer concentration with time (obtained by integration of the spectra) was used to measure the extent of reaction α (defined as $\alpha = \text{trans}/(\text{cis} + \text{trans})$), where $\alpha = 0$ corresponds to pure *cis* isomer (reactant) and $\alpha = 1$ corresponds to pure *trans* isomer (product).

In our case we followed the isomerization at four different temperatures (65, 70, 75, and 80 °C). In Figure 2 the bridging

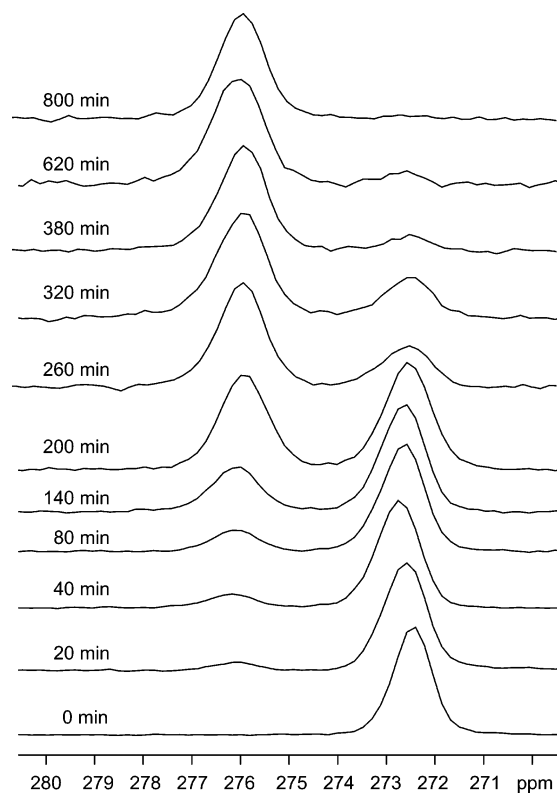


Figure 2. Bridging carbonyl region of the ^{13}C CPMAS spectra of $[(\eta^5\text{-C}_5\text{H}_5)\text{Fe}(\mu\text{-CO})(\text{CO})]_2$ at different heating times.

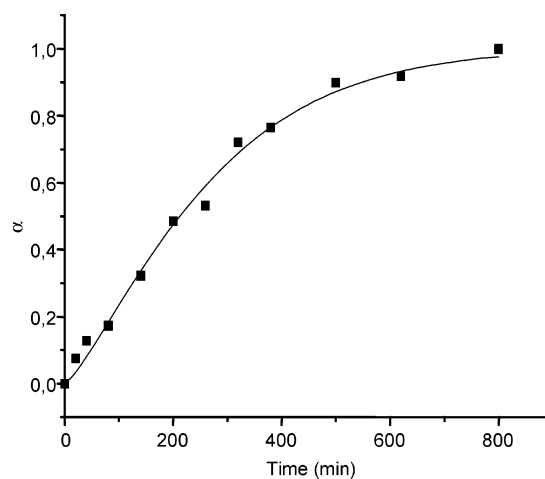


Figure 3. Isomerization kinetics of $\text{cis}-[(\eta^5\text{-C}_5\text{H}_5)\text{Fe}(\mu\text{-CO})(\text{CO})]_2$ at 65 °C.

carbonyl region of the spectra with different heating times for the isotherm at 65 °C is reported.

In order to evaluate which mechanism for this transition is operative over the temperature range examined, the fractional completion, α , is plotted as a function of time for the four isotherms. As an example in Figure 3 the results obtained at 65 °C are reported. The resulting conversion–time curves have the typical sigmoid shape characteristic for most solid-state conversions that are not diffusion-controlled.

A simple and general method for the analysis of this type of isotherms has been introduced by Avrami–Erofe'ev²⁴ with the so-called Avrami–Erofe'ev rate law:

$$[-\ln(1 - \alpha)]^{1/n} = kt \quad (1)$$

The model proposed by Avrami–Erofe'ev assumes that “germ nuclei” of the reaction product are distributed randomly

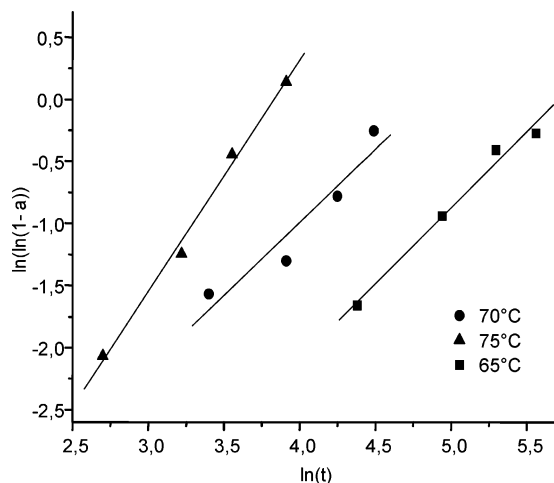


Figure 4. Sharp and Hancock's plot of $\ln[-\ln(1-\alpha)]$ vs $\ln(t)$ of the isomerization according to eq 2.

within the solid; following the nucleation event, the grains grow until the transformation is complete. In this case, the shape of the kinetic plots is analyzed into four regions: (i) an induction period ($0.1 < \alpha < 0.15$); (ii) an acceleratory region ($0.15 < \alpha < 0.5$); (iii) a deceleratory region ($0.5 < \alpha < 1$); and (iv) the completion ($\alpha = 1$). The nucleation prevails in the induction period, and the acceleratory region tends to be dominated by growth. The termination of growth results in the deceleratory region.

Following eq 1 the experimental data recorded at 65 °C (Figure 3) can be fit with $n = 1.3$, typical of a nucleation and a one-dimensional growth mechanism.²⁴

A similar approach exploits Sharp and Hancock's equation:²⁵

$$\ln[-\ln(1-\alpha)] = n \ln(t) + b \quad (2)$$

where the exponent term n is equivalent to the gradient n of the Avrami–Erofe'ev plot.

Sharp and Hancock's plot, when linear over the interval $0.15 < \alpha < 0.5$, is diagnostic of the reaction mechanisms.²⁶ Briefly, $n \approx 0.5$ is associated with a diffusion-controlled reaction, for $n = 1$ a phase-boundary control is appropriate, while $n = 1-2$, $n = 2-3$, and $n = 3-4$ are consistent with nucleation and growth via a one-dimensional, two-dimensional, and three-dimensional growth, respectively.

In an isokinetic process the exponential n term in Avrami–Erofe'ev equation (eq 1) does not change, and thus Sharp and Hancock's lines are identical in slope at different temperatures. When the reaction mechanism changes with temperature, the analysis will indicate either a progressive change in mechanism (the n exponential term changes gradually as well as the slope of the lines) or an instantaneous change (the n value and the slope of the lines change dramatically).

In our case, Avrami–Erofe'ev fitting provides different n values for the different temperatures. In particular we have found $n = 1.3$ for the isotherm at 65 °C, $n = 1.3$ for the isotherm at 70 °C, $n = 1.7$ for the isotherm at 75 °C, and $n = 4$ for the highest temperature isotherm (80 °C). Indeed we can argue that the solid-state *cis*–*trans* isomerization is not isokinetic. Similar

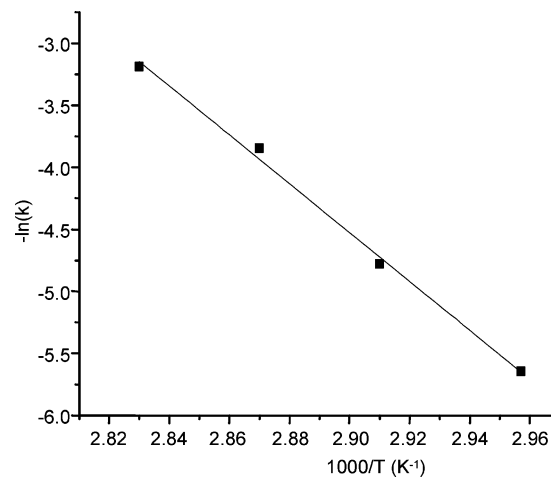


Figure 5. Arrhenius plot used for obtaining the activation energy of the isomerization process.

results have been obtained with Sharp and Hancock's plots (Figure 4) of $\ln[-\ln(1-\alpha)]$ vs $\ln(t)$, whose slope changes with the temperature.

The isotherms at 65, 70, and 75 °C are associated with slope values of 1.2, 1.2, and 1.9, respectively. Unfortunately we cannot report the plot for the last isotherm because the fast rate of reaction prevented the collection of a sufficient number of points in the range $0.15 < \alpha < 0.5$. Since all the data are in agreement with Avrami–Erofe'ev analysis, we assumed for this isotherm $n = 4$.

These results are in agreement with a reaction mechanism that passes from nucleation and growth via a one-dimensional growth, to nucleation and growth via a three-dimensional growth by increasing the reaction temperature.

Other known algebraic expressions, listed by Gotor et al.,²⁷ usually used for describing the most common mechanisms in solid-state processes were found less suitable for the analysis of this isomerization reaction.

The kinetic constant value was calculated for the four isotherms, and by using the resulting Arrhenius plot (Figure 5), a value of 164 ± 7 kJ/mol for the activation energy (E_a) of the isomerization process in the solid state has been obtained. This value is in agreement with reported E_a calculated for transformations occurring in the solid state.²⁸

The isomerization prevented us from studying the terminal–bridge carbonyl exchange process in the *cis* isomer. The same behavior has been observed for the solution state where the *cis* isomer undergoes preferentially the isomerization process than the terminal–bridge carbonyl exchange.¹⁹ Indeed the latter mechanism would require a rotation about the Fe–Fe bond of one of the $\text{Fe}(\eta^5\text{-C}_5\text{H}_5)(\text{CO})_2$ units by $2\pi/3$ or $-4\pi/3$ (thus effecting the enantiomerization $1c_c \rightleftharpoons 1c_{c^*}$; see Scheme 1). Nevertheless, such exchange can be well observed in the stable *trans* form by variable-temperature ¹³C CPMAS NMR. In Figure 6 selected carbon SS NMR spectra are reported for a temperature range varying from 25 to 85 °C.

The spectral features described above are clearly consistent with dynamic behavior of the *trans* isomer involving bridge–terminal exchange.

(24) (a) Avrami, M. *J. Chem. Phys.* **1941**, *9*, 177–184. (b) Erofe'ev, B. V. C. R. *Dokl. Akad. Nauk SSSR* **1946**, *52*, 511–514.

(25) Sharp, J. H.; Hancock, J. D. *J. Am. Ceram. Soc.* **1972**, *55*, 74.

(26) (a) Custelcean, R. *Thermochim. Acta* **2002**, *388*, 143–150. (b) Saikia, N.; Sengupta, P.; Gogoi, P. K.; Borthakur, P. *Ch. Appl. Clay Sci.* **2002**, *22*, 93–102.

(27) Gotor, F. J.; Criado, J. M.; Malek, J.; Koga, N. *J. Phys. Chem. A* **2000**, *104*, 10777.

(28) (a) Bala, M. D.; Levendis, D. C.; Coville, N. J. *J. Organomet. Chem.* **2006**, *691*, 1919–1926. (b) Finze, M.; Bernhardt, E.; Willner, H.; Lehmann, C. W. *J. Am. Chem. Soc.* **2005**, *127*, 10712–10722. (c) Eslami, A. *Thermochim. Acta* **2004**, *409*, 189–193.

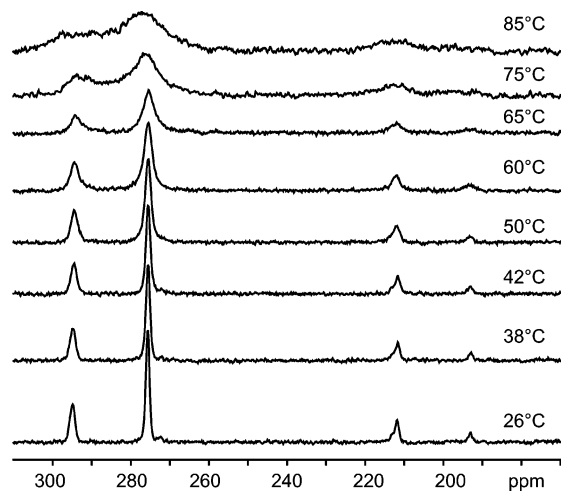


Figure 6. Selected variable-temperature ^{13}C CPMAS NMR spectra of $\text{trans}-[(\eta^5\text{-C}_5\text{H}_5)\text{Fe}(\mu\text{-CO})(\text{CO})_2]$. Bridging and terminal carbonyl region only.

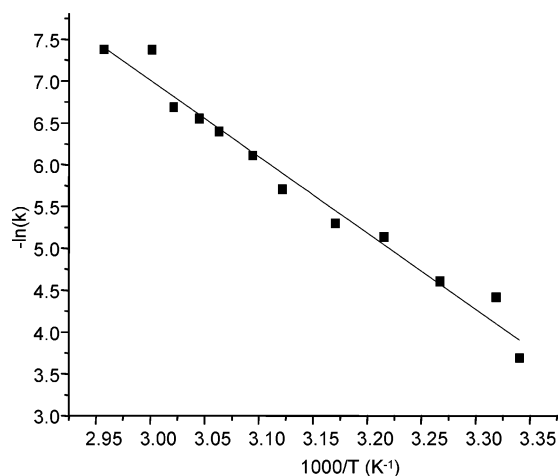


Figure 7. Arrhenius plot for the activation energy of the carbonyl exchange process in the *trans* isomer in the solid state.

By simulation of the spectra the kinetic constant values for the exchange process have been determined at different temperatures, yielding the Arrhenius plot shown in Figure 7.

The calculated activation energy for the carbonyl exchange process in the *trans* isomer in the solid state is 76 ± 3 kJ/mol.

We can assert that in both the solid and solution state the isomerization mechanism requires a higher E_a with respect to the carbonyl exchange mechanism in the *trans* form (164 and 76 kJ/mol in the solid state compared to 46.8 and 29.7 kJ/mol in solution¹⁹). Moreover, in both cases the bridge-terminal carbonyl exchange process for the *cis* isomer has a higher E_a value; that is, the carbonyl exchange takes place only through the *cis-trans* isomerization process. Therefore, since the E_a trend is in accordance with that obtained for the liquid state by Farrugia et al.,¹⁹ we surmise that the same mechanism may be responsible for the isomerization in solution as well as in the solid state. Thus, in both phases the formation of an all-terminal carbonyl intermediate can occur, and then the isomerization takes place via the rotation of the $\text{Fe}(\eta^5\text{-C}_5\text{H}_5)(\text{CO})_2$ unit, followed by the reorganization of the ligands to re-form carbonyl bridges. No rotation is necessary for the bridging-terminal carbonyl exchange process in the *trans* isomer. The intermediate is not observed in the spectra, due to its very short lifetime. The rigid constraint caused by the crystal packing is the reason for the higher activation energy found for the solid-state process.

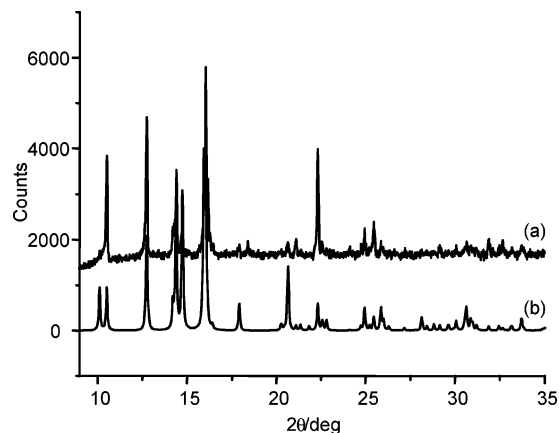


Figure 8. Comparison between the X-ray diffraction powder pattern measured at room temperature on a sample of the *cis* isomer (a) and that calculated on the basis of the single-crystal structure (b).

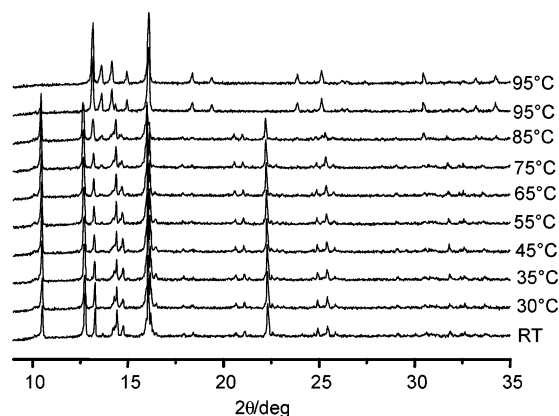


Figure 9. Variable-temperature X-ray diffraction patterns measured on a polycrystalline sample of the *cis* isomer measured between rt and 95 °C.

Variable-Temperature X-ray Diffraction Experiments. A sample of the *cis* isomer obtained as indicated above was subjected to variable-temperature X-ray diffraction measurements. The sample was unambiguously identified as pure *cis* isomer by comparing the X-ray powder diffraction pattern measured at room temperature with that calculated on the basis of the single-crystal structure (see Figure 8).

Figure 9 shows the diffraction pattern measured in the range rt to 95 °C on a pure sample of *cis* isomer at steps of 10 deg. It can be easily appreciated how the pattern is constant up to ca. 75 °C, showing persistence of the *cis*-form.

Above 75 °C the diffraction peaks suddenly change to those of the *trans* isomer. The sample was also left standing at 95 °C for 10 min before remeasuring the diffraction pattern, showing that no further change took place. Cooling the sample to room temperature retains the *trans* isomer pattern, confirming the nonreversible nature of the *cis-trans* solid-state isomerization.

Conclusions

With this study we have gained further insights in one of the most studied dynamical process of organometallic chemistry. The fluxional behavior of $[(\eta^5\text{-C}_5\text{H}_5)\text{Fe}(\mu\text{-CO})(\text{CO})_2]$ has constituted a matter of investigation and debate for a long time. We have provided evidence by solid-state methods that the *cis-trans* isomerization process known to take place in solution occurs, though irreversibly, in the solid state. A polycrystalline

sample of the *cis* isomer transforms rapidly and quantitatively into that of a *trans* isomer upon heating. The activation energy barrier estimated for the isomerization is 164 ± 7 kJ/mol. The process, followed by ^{13}C CPMAS, can be described with a nucleation and growth mechanism. The kinetic data fit well with a first-order Avrami–Erofe'ev equation, and the comparison with the Sharp–Hancock analysis confirms that the process is nonisokinetic, passing from a one-dimensional to a three-dimensional growth.

The bridge–terminal carbonyl exchange mechanism studied by means of VT ^{13}C CPMAS experiments provides an activation energy of 76 ± 3 kJ/mol. Thus, as in the solution state, the carbonyl exchange mechanism in the *trans* form having a lower E_a is independent of the isomerization process. On the contrary, in the *cis* isomer it occurs only through the *cis*–*trans* isomerization because it requires an enantiomerization $1c_c \leftrightarrow 1c_c^*$, i.e., a rotation about the Fe–Fe bond by $2\pi/3$ or $-4\pi/3$, with a high E_a .

It has been observed that in the solid state, as in solution, the trend of the E_a of the studied processes is the following: E_a bridging–terminal $(\text{CO})_{\text{trans}}$ exchange $< E_a$ *cis*–*trans* isomerization $< E_a$ bridging–terminal $(\text{CO})_{\text{cis}}$ exchange. On this basis one can surmise that the mechanism described by Farrugia et al.¹⁹ and reported in Scheme 1 occurs also in the solid state.

Experimental Section

All reagents were purchased from Aldrich and used without further purification.

^{13}C -Enrichment. ^{13}C -enriched $[(\eta^5\text{-C}_5\text{H}_5)\text{Fe}(\mu\text{-CO})(\text{CO})]_2$, with about 20% ^{13}C enrichment, was prepared by direct exchange of ^{13}C with the appropriate metal carbonyl in heptane (purified by

standard techniques²⁹) solution at 80 °C for 3 days.³⁰ ^{13}C (99% enriched) was purchased from Isotec, Miamisburg, OH.

To obtain the *cis* form, the ^{13}C -enriched compound was dissolved in a small quantity of CH_2Cl_2 . The solution was cooled at approximately -50 °C in an acetone bath, and the solvent stripped out with a strong nitrogen flow.

The isomerization process was followed by heating the sample in an oven set at the isotherm temperature. The sample was heated progressively, and the extent of the reaction checked by collecting the NMR spectra.

Solid-State NMR Spectroscopy. ^{13}C CPMAS NMR spectra were acquired on a JEOL GSX 270 WB operating at 67.8 MHz for ^{13}C . A standard cross-polarization pulse sequence has been used with a contact time of 5 ms and a 90° pulse of 4.5 μs . Typically, 32 transients were collected for each spectrum with a pulse delay of 10 s. Samples were packed in 5 mm zirconia rotors with a typical sample volume of 120 μL . MAS rates varied from 5 to 6 kHz. The sample temperature in the variable-temperature experiments was verified from the chemical shift of $^{207}\text{Pb}(\text{NO}_3)_2$, as described by Bielecki and Burum.³¹

The exchange process involving bridging and terminal carbonyls in the *trans*- $[(\eta^5\text{-C}_5\text{H}_5)\text{Fe}(\mu\text{-CO})(\text{CO})]_2$ derivative was simulated with the gNMR V4.1 program.³² The intensity of the bridging carbonyls is approximately 3 times the terminal signal due to the large difference in their anisotropies.²⁰ For the simulation we assumed that this ratio was not substantially modified since in the temperature range under investigation only a negligible change in the CSA was detected by spinning sideband analysis.

X-ray Diffraction. X-ray powder diffractograms were collected on a Pananalytical X'Pert PRO automated diffractometer with Cu $K\alpha$ radiation and an X'Celerator detector equipped with an Anton Paar TTK 450 low-temperature camera.

Acknowledgment. We thank MIUR (PRIN 2004 and FIRB2001) and the University of Torino and Bologna for financial support.

OM061103E

(29) Armarego, W. F.; Perrin, D. D. *Purification of Laboratory Chemicals*; Butterworth Heineman: New York, 1998.

(30) Bricker, J. C.; Payne, M. W.; Shore, S. G. *Organometallics* **1987**, *6*, 2.

(31) Bielecki, A.; Burum, D. P. *J. Magn. Reson.* **1995**, *116*, 215–220.

(32) Budzelaar P. H. M. *gNMR version 4.1*; Adept Scientific plc, 1999.